Inorganic Chemistry

Article

pubs.acs.org/IC

Hypoelectronic Dimetallaheteroboranes of Group 6 Transition Metals Containing Heavier Chalcogen Elements

Kiran Kumarvarma Chakrahari, Arunabha Thakur, Bijan Mondal, V. Ramkumar, and Sundargopal Ghosh*

Department of Chemistry, Indian Institute of Technology Madras, Chennai 600 036, India

Supporting Information

ABSTRACT: We have synthesized and structurally characterized several dimetallaheteroborane clusters, namely, *nido*-$[(Cp^*Mo)_2B_4SH_6]$, **1**; *nido*-$[(Cp^*Mo)_2B_4SeH_6]$, **2**; *nido*-$[(Cp^*Mo)_2B_4TeClH_5]$, **3**; $[(Cp^*Mo)_2B_5SeH_7]$, **4**; $[(Cp^*Mo)_2B_6SeH_8]$, **5**; and $[(CpW)_2B_5Te_2H_5]$, **6** ($Cp^* = \eta^5$-C_5Me_5, $Cp = \eta^5$-C_5H_5). In parallel to the formation of **1**−**6**, known $[(CpM)_2B_5H_9]$, $[(Cp^*M)_2B_5H_9]$, (M = Mo, W) and *nido*-$[(Cp^*M)_2B_4E_2H_4]$ compounds (when M = Mo; E = S, Se, Te; M = W, E = S) were isolated as major products. Cluster **6** is the first example of tungstaborane containing a heavier chalcogen (Te) atom. A combined theoretical and experimental study shows that clusters **1**−**3** with their open face are excellent precursors for cluster growth reactions. As a result, the reaction of **1** and **2** with $[Co_2(CO)_8]$ yielded clusters $[(Cp^*Mo)_2B_4H_4E(\mu_3\text{-}CO)Co_2(CO)_4]$, **7**−**8** (**7**: E = S, **8**: E = Se) and $[(Cp^*Mo)_2B_3H_3E(\mu\text{-}CO)_3Co_2(CO)_3]$, **9**−**10** (**9**: E = S, **10**: E = Se). In contrast, compound **3** under the similar reaction conditions yielded a novel 24-valence electron triple-decker sandwich complex, $[(Cp^*Mo)_2\{\mu\text{-}\eta^6\text{:}\eta^6\text{-}B_3H_3TeCo_2(CO)_5\}]$, **11**. Cluster **11** represents an unprecedented metal sandwich cluster in which the middle deck is composed of B, Co, and Te. All the new compounds have been characterized by elemental analysis, IR, ^1H, ^{11}B, ^{13}C NMR spectroscopy, and the geometric structures were unequivocally established by X-ray diffraction analysis of **1**, **2**, **4**−**7**, and **9**−**11**. Furthermore, geometries obtained from the electronic structure calculations employing density functional theory (DFT) are in close agreement with the solid state structure determinations. We have analyzed the discrepancy in reactivity of the chalcogenato metallaborane clusters in comparison to their parent metallaboranes with the help of a density functional theory (DFT) study.

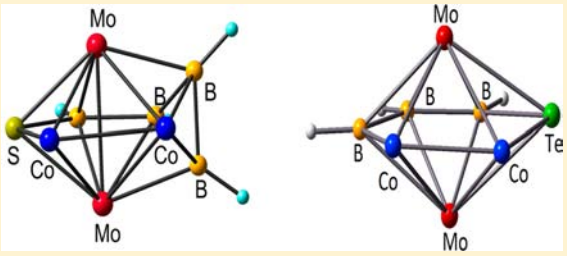

INTRODUCTION

Boron, being the only nonmetal element in group 13, forms a number of different clusters both with main group and transition metal elements.[1] Over the past few decades, extensive efforts have been devoted toward the synthesis of mixed-metal chalogenide clusters of high nuclearity.[2,3] An area of continuing importance in polyhedral metallaborane chemistry is the development of new and efficient methods, leading to expanded cluster cage. Although for the past few decades Fehlner and others have worked on boron-transition metal clusters,[4−9] development in this area has been slow. Only the most stable/least reactive compounds are characterized limiting the scope of this field of chemistry, particularly when early transition metals are of interest. However, because of the availability of few synthetic procedures that are of great promise for the synthesis of metallaborane compounds,[9,10] the chemistry of this sub area of transition metal complexes of boron have received significant attention from both the structure/bonding and the reactivity perspective. As a result, recent years have witnessed significant development of many interesting polyhedral cage structures, which includes the expansions of single clusters beyond icosahedral cage to give species with 13, 14, 15, or 16 vertices.[11−13] In addition, the study of metallaboranes has flourished and recently has been finding applications in other areas of chemistry.[14]

Although several approaches are available for cluster growth reaction in metallaborane chemistry, the reaction pathway often leads to the formation of a range of products with varying M:B ratios and in low yields.[15] Many times, it is rather challenging to generate a single cage cluster with higher number of vertices of pure boron and metal. However, a combination of metal, boron, and other main group elements often generate novel geometry. Recently, we have demonstrated that compounds of the type $[(Cp^*Mo)_2B_4H_4E_2]$ (E = S, Se, Te) are useful metal synthons for cubane-type clusters.[16] Further, a combined theoretical (density functional theory (DFT)) and experimental study reveals that the reactivity of dimolybdaborane $[(Cp^*Mo)_2B_5H_9]$ with various metal carbonyls increases upon the replacement of one of the open face boron vertices by chalcogen atoms.[17] For example, the reaction of **3** with $[Co_2(CO)_8]$ at room temperature yielded a byproduct which is a member of a novel class of triple-decker complexes.[18] Herein, we report the synthesis, structural characterization, and electronic structure of several novel hypoelectronic metallaheteroboranes.

Received: February 19, 2013
Published: July 2, 2013

 © 2013 American Chemical Society dx.doi.org/10.1021/ic400432v | *Inorg. Chem.* 2013, 52, 7923−7932

Scheme 1. Synthesis of Dimetallaheteroborane Clusters 1−6

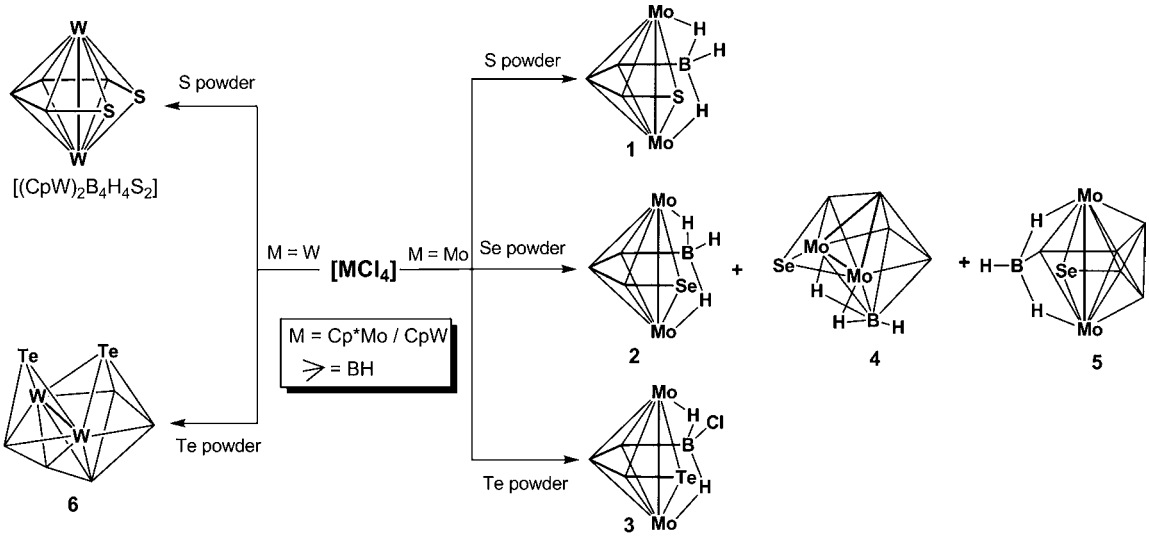

Table 1. Comparison of Structural Parameters and ^{11}B Chemical Shifts of 1−3 and Other Related Clusters

entry	d[M−M] (Å)	d[B−B] (Å)	^{1}H NMR (M−H−B) δ [ppm]	^{11}B NMR δ [ppm]	calculated (DFT) ^{11}B NMR	reference
1	2.78	1.78	−10.4	101.1, 76.7, 40.3, 10.1	109.9, 71.9, 37.2, 4.8	this work, (17a)
2	2.77	1.99	−10.4	100.7, 76.7, 41.8, 16.8	104.9, 68.5, 35.8, 12.4,	this work
3	2.84	1.79	−6.60	95.4, 73.1, 40.7, 26.6	105.2, 68.2, 37.1, 26.6	16b
$[(Cp^*Mo)_2B_4H_6S_2]$	2.63	1.69		81.8, −4.1	73.3, −8.5	17b, 19a
$[(Cp^*Mo)_2B_4H_6Se_2]$	2.66	1.71		81.8, 4.2	90.3, −1.69	19a
$[(Cp^*Mo)_2B_4H_6Te_2]$	2.69	1.79		81.3, 11.6	92.3, 7.0	17b, 19a
$[(Cp^*Mo)_2B_4H_5SePh]$	2.81	1.74	−6.81	98.7, 77.5, 42.0, 28.2		19b

RESULTS AND DISCUSSION

Synthesis and Characterization of 2, 4−6. As shown in Scheme 1, thermolysis of *in situ* generated intermediates, obtained from the reaction of $[Cp^*MoCl_4]$ or $[CpWCl_4]$ with $LiBH_4$·thf, in presence of chalcogen powders led to the formation of clusters **1**−**6**. Although compounds **2**, **4**, and **5** were produced in a mixture, these compounds can be separated by preparative thin-layer chromatography (TLC), allowing the characterization of pure materials. Details of the characterization of compounds **2** and **4**−**6** are given below.

$[(Cp^*Mo)_2B_4SeH_6]$, 2. Compound **2** was isolated as an orange solid in 25% yield. The spectroscopic data of **2** is comparable with that of **1** and **3** reported earlier[17,16b] and consistent with its solid state structure (determined by X-ray diffraction). The ^{11}B NMR spectrum of **2** indicates the presence of four boron resonances at δ = 100.7, 76.7, 41.8, and 16.8 in an intensity ratio of 1:1:1:1. The resonance at δ = 16.8 ppm has been assigned to the boron that is attached to selenium atom. As shown in Table 1, the chemical shift of that particular boron appeared between the chemical shift observed for the S and Te analogues. Interestingly, a similar trend has also been observed in compounds $[(Cp^*Mo)_2B_4H_4E_2]$ (E = S, Se, Te).[17,19] The solid state structure of compound **2** can be defined as a bicapped trigonal bipyramid (Supporting Information, Figure S1). The Mo−Mo bond distance in cluster **2** is comparable with that of **1** (Supporting Information, Figure S2) and **3**. The ^{11}B chemical shifts of **1**−**3** match with those calculated using the gauge-independent atomic orbital density functional theory [GIAO−DFT] method at the B3LYP (SDD, DGDZVP) level and referenced to BF_3·OEt_2 (Table 1). This indeed provides a stringent test to the validity of the calculated electronic structures of the complexes **1**−**3**.

$[(Cp^*Mo)_2B_5SeH_7]$, 4. Compound **4** was isolated as a yellow solid in 8% yield. The ^{11}B NMR spectrum of **4** shows five distinct boron environments at δ = 86.4, 33.7, 32.0, 20.3, and −3.2 ppm. The chemical shift at −3.2 ppm may be attributed to the unique boron which is attached to Se atom. The ^{1}H NMR spectrum shows one signal for two Mo−H−B protons.

The framework geometry of **4** was unambiguously established by its solid state structure determination. As shown in Figure 1, the structure of **4** can be viewed as a bicapped trigonal prism with C_s symmetry, in which $\{Mo_2B_4\}$ occupies the core vertices of a trigonal prism and B1 is capping the Mo_2B_2 square plane. Further, it has a single degree 3 vertex (μ-Se) capping the Mo_2B triangular face of an underlying capped trigonal prism. On the basis of the capping principle, the skeletal electron count is determined by the central polyhedron (i.e., Mo_2B_4 trigonal prism) that amounts to seven skeletal electron pairs (sep), required for the bicapped trigonal prism. Thus, **4** obeys the electron-counting rules[20] for the observed geometry. Alternatively, the structure of **4** can be viewed as a bicapped octahedron where B5 capped one trigonal face {Mo1B4Mo2} of octahedron {Mo1Mo2B1B2B3B4}. One of the resulting trigonal faces, {Mo1Mo2B5} is then further capped by Se in μ_3-fashion. The Mo1−Mo2 bond length of 2.777(5) Å is shorter than that observed in $[(Cp^*Mo)_2B_5H_9]$[21] (2.8012(16) Å) and other molybdaheteroborane clusters.[19] The shortening of the Mo−Mo bond might arise from the effect of the selenium atom that withdraws electron density from the cluster. The B−Se bond length of 1.905(8) Å is

dx.doi.org/10.1021/ic400432v | Inorg. Chem. 2013, 52, 7923−7932

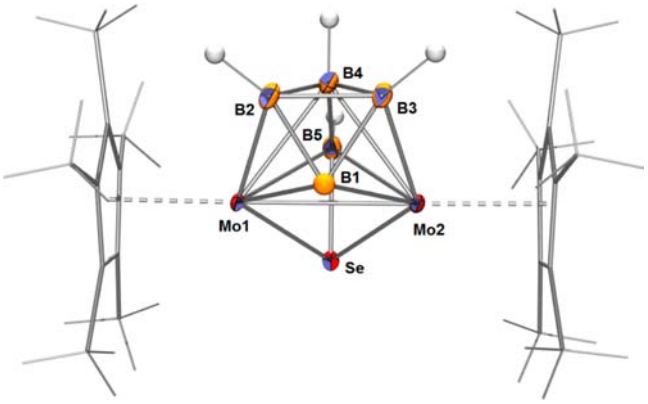

Figure 1. Molecular structure and labeling diagram for **4**. The open face boron and selenium atoms are disordered over two orientations (B1, B1′) and (Se1, Se1′) in the ratio of (0.7, 0.3). Selected bond lengths (Å) and angles (deg): Mo(1)−Mo(2) 2.777, Mo(1)−B(1) 2.354(9), Se(1)−B(5) 1.905(8), B(1)−B(2) 1.703(14), B(2)−B(3) 1.683(13), B(2)−B(4) 1.680(15), B(3)−B(4) 1.694(16), Se(1)−Mo(2) 2.565(8); Mo(1)−Se(1)−Mo(2) 65.57(2), Mo(2)−B(5)−Se(1) 72.9(2).

comparable to other metallaselenaboranes, for example, 1.93(3) Å and 2.025(3) Å in $[(Cp^*Mo)_2B_4H_4Se_2]$ and $[(Cp^*Mo)_2B_5H_8SePh]$, respectively.[19,22]

$[(Cp^*Mo)_2B_6SeH_8]$, 5 and $[(CpW)_2B_5Te_2H_5]$, 6. Compounds **5** and **6** were isolated as an orange and a brown solid in 11% and 7% yield, respectively. The spectroscopic data of **5** and **6** are fully consistent with their solid state structures (Figure 2).

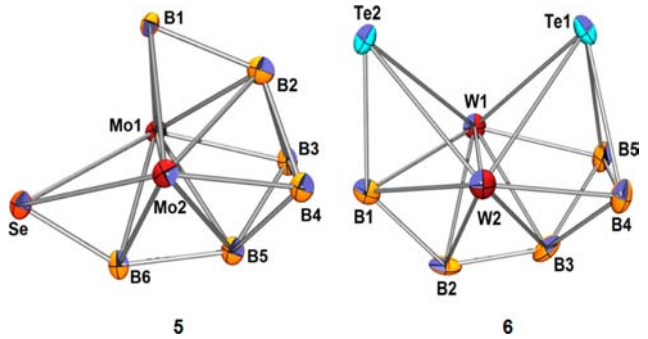

Figure 2. Molecular structures and labeling diagram for **5** and **6**. (Cp* and Cp ligands are not shown for clarity) **5**: The μ_3-Se atom is disordered over two orientations (Se1, Se2) in the ratio of 0.42:0.58, respectively. Selected bond lengths (Å) and angles (deg), **5**: Mo(1)−Mo(2) 2.779, Mo(1)−B(2) 2.400(16), B(6)−Se(1) 1.789, Se(1)−Mo(1) 2.719(3), B(2)−B(4) 1.84(2), B(1)−B(2)1.856(19), B(5)−B(6) 1.837(18), B(4)−B(5) 1.735(17); Mo(1)−Se(1)−Mo(2) 61.72(6), B(1)−Mo(2)−Se(1) 81.9(6); **6**: W(1)−W(2) 2.771(7), W(1)−B(2) 2.228(9), B(1)−Te(2) 2.133(17), B(4)−Te(1) 2.309(13), Te(1)−W(2) 2.786(8), B(1)−B(2) 1.70(2), B(3)−B(4) 1.756(19); W(1)−Te(1)−W(2) 59.89(2).

Consistent with the solid state structure (determined by X-ray diffraction), the ^{11}B NMR spectrum of **5** shows the presence of five boron environments appear each at δ = 95.4, 78.2, 14.1, 6.5, and −10.9 ppm in an intensity ratio of 1:2:1:1:1. Compound **6** shows four boron chemical shifts in the ratio of 1:1:2:1 at 87.2, 77.5, 44.1, and −12.0 ppm. The upfield chemical shift at δ −10.9 ppm for **5** and −12.0 for **6**, accounted for four coordinated boron attached to Se (**5**), and Te (**6**). In the high-field region of the ^{1}H NMR spectrum of **5**, a sharp signal is observed at δ −9.18 ppm, which could be assigned for Mo-*H*-B.

Single crystals suitable for X-ray diffraction analysis of **5** and **6** were obtained from a hexane solution at −5 °C, thus allowing for their structural characterization. All the B−B, W−B, and W−Te bond distances are in the normal range. However, the W−W distance of 2.7719(7) Å falls in the range associated with a W−W single bond,[23] and is significantly shorter than that in the other tungstaborane cluster.[24] This may be due to the lesser tendency of boron and tellurium atoms to form polarized bonds that have a localized two-center character resulting in the observed distances.[25,26] The overall geometry of clusters **5** and **6** is intriguing. The observed geometry of **5** can be viewed as a fused cluster in which a capped octahedron {Mo1-Mo2B1B2B3B4B5} is fused to a trigonal bipyramidal unit {Mo1Mo2B5B6Se} via a common face {Mo1Mo2B5}. On the other hand, in **6** a capped trigonal bipyramid {W1W2B1B2B3Te2} unit is fused to an octahedral unit {W1W2B_3B4B5Te1} with three atoms (W1, W2 and B3) held common between the two sub clusters. Note that there are only few crystallographically characterized clusters known, (Chart 1, *a*−*d*) where octahedral units are fused via a triangular face. Alternatively the geometry of cluster **5** can be interpreted as a tricapped trigonal prism where Mo1, Mo2, B6, B5, B4, and B3 occupy the vertices of the core trigonal prism. Further, a square face, {Mo1Mo2B4B3} and a trigonal face {Mo1Mo2B6} is capped by B2 and μ_3-Se atoms, respectively. The resulting {Mo1Mo2B2} face in turn is capped by a B1 atom. In a similar fashion, cluster **6** can also be viewed as tricapped trigonal prism, where the Te atom capped one of the resulting trigonal faces (W1W2B1) of the bicapped trigonal prism. Thus, clusters **5** and **6** may be considered as geometrical isomers. Considering a trigonal prism, both **5** and **6** contain 7 sep as required for this geometry.

Reactivity of 1−3 with $[Co_2(CO)_8]$. The cluster expansion reactions of main group and transition metal polyhedral metallaboranes using metal carbonyl fragments are well-documented;[29] however, examples proceeding in high yield with clean and well-defined stoichiometry are limited. Earlier it has been shown by Fehlner and co-workers that the reaction of $[(Cp^*M)_2B_5H_9]$ (M = Cr, Mo or W) with $[Co_2(CO)_8]$ led to decomposition of starting material. As a result, we have carried out the reactions of **1**−**3** with $[Co_2(CO)_8]$ at ambient temperature, which resulted in a range of mixed-metal-laheteroborane clusters. This result shows that the reactivity of $[(Cp^*Mo)_2B_5H_9]$ with $[Co_2(CO)_8]$ enhances manyfold if one of the boron vertices is replaced by a chalcogen atom. Quantum-chemical calculations using DFT methods at the B3LYP (SDD, DGDZVP) level of theory have been carried out to find out this unusual reactivity pattern. The DFT molecular orbital study shows a significant destabilization of the highest occupied molecular orbitals (HOMOs) of clusters **1**−**3** that suggests a higher reactivity compared to their parent molecule, $[(Cp^*Mo)_2B_5H_9]$ (Figure 3). This destabilization of HOMOs may be due to the introduction of π-donor chalcogen ligands into the clusters.[17b] Furthermore, a realistic indicator, Ionization Potential (IP) energy, has also been computed and used as a probe to explain the reactivity pattern. Both the DFT-computed vertical and adiabatic first IP are shown in Figure 4. The computed IP value, about 6.0 eV, is consistent with the high thermodynamic stability of compounds **1**−**3**. Because of the significant geometry change upon ionization, the vertical

dx.doi.org/10.1021/ic400432v | *Inorg. Chem.* 2013, 52, 7923−7932

Chart 1. Face Fused Clusters[a]

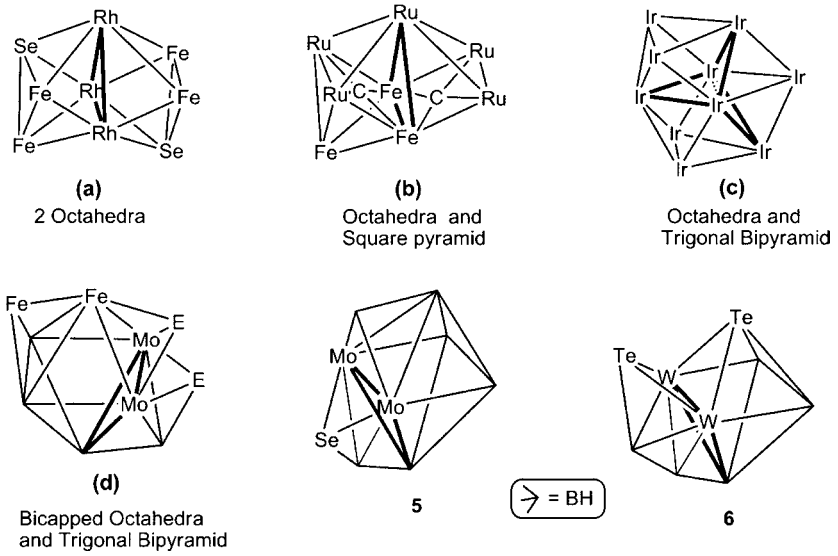

[a](**a**) $[PPh_4]_2[Fe_3Rh_4Te_2(CO)_{15}][PPh_4]_2$, two octahedral units fused by a common Rh_3 face;[27a] (**b**) $[Fe_3Ru_3(\mu_6\text{-C})(\mu_5\text{-C})(\mu\text{-}PPh_2)_2(CO)_{17}]$,[27b] square-pyramidal $Fe_2Ru_3(\mu_5\text{-C})$ unit fused to an octahedral $Fe_3Ru_3(\mu_6\text{-C})$ by Fe_2Ru face; (**c**) $[Ir_{10}(CO)_{21}]^{2-}$ formed by face-sharing fusion of two octahedra and a trigonal bipyramid;[27c] and (**d**) $[(Cp^*Mo)_2B_4H_4E_2Fe(CO)_2Fe(CO)_3]$,[28] bicapped octahedron unit fused with trigonal bipyramid.

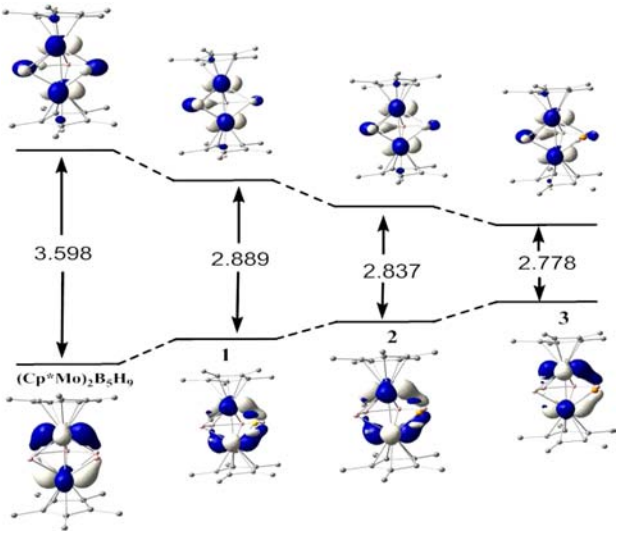

Figure 3. Molecular orbital diagrams of $[(Cp^*Mo)_2B_5H_9]$ and **1**−**3**.

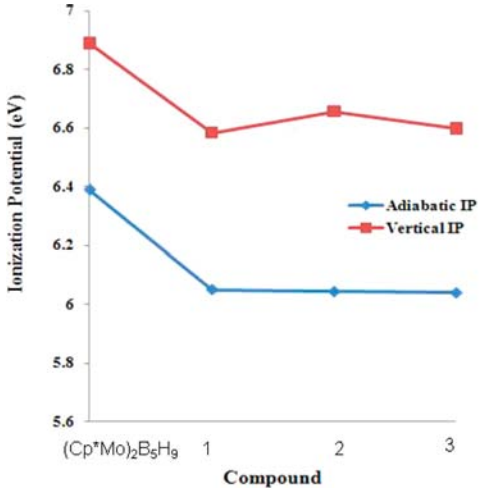

Figure 4. Vertical and adiabatic first IPs (eV) for $[(Cp^*Mo)_2B_5H_9]$ and **1**−**3**.

curve is a few tenths of an electron volt higher in energy relative to the adiabatic one.

The room temperature reaction of $[Co_2(CO)_8]$ with **1** led to the isolation of compounds $[(Cp^*Mo)_2B_4H_4E(\mu_3\text{-CO})\text{-}Co_2(CO)_4]$, **7** and **8** (**7**: E = S, **8**: E = Se) whereas with **2**, compounds $[(Cp^*Mo)_2B_3H_3E(\mu\text{-CO})_3Co_2(CO)_3]$ **9** and **10** (**9**: E = S, **10**: E = Se) have been isolated. In contrast, compound **3** under the similar reaction conditions, yielded a novel 24 valence electron triple-decker complex, $[(Cp^*Mo)_2\{\mu\text{-}\eta^6\text{:}\eta^6\text{-}B_3H_3TeCO_2(CO)_5\}]$, **11** (Scheme 2). The details of characterization of compounds **7**−**11** have been discussed as follows.

Clusters 7 and 8. Compounds **7** and **8** have been isolated as orange solids in 20% and 10% yield respectively. The molecular structure of **7**, shown in Figure 5, is seen to be consistent with the solution spectroscopic data. Unfortunately, all of our efforts to grow single crystals of **8** resulted in weakly diffracting material. Nevertheless, the structure of **8** was confirmed by comparing its spectroscopic data with that of its sulfur analogue **7**. Cluster **7** does not display the structural motif expected for a *closo*-nine-vertex cluster, that is, a tricapped trigonal prism. Moreover, the Mo centers are separated by 2.922 Å, within the range normally associated with Mo−Mo single bonds.[30,31] All the Mo−B, Mo−S, B−S, and B−B bond lengths are in the range normally associated with bonding interactions. The carbonyls were located in the difference map, and their presence was confirmed by IR spectroscopy. The triply bridged carbonyl is located on the {Co1Co2Mo1} face, and each of the cobalt atoms has two terminal carbonyl ligands.

Consistent with the solid state structure (determined by X-ray diffraction), the ^{11}B NMR spectra of both **7** and **8** show the presence of four boron environments in the ratio of 2:1:1, at δ = 102.6, 77.2, 35.4 ppm for **7** and δ = 101.8, 77.4, 38.6 ppm for **8**. The ^1H NMR spectra of **7** and **8** show a single sharp peak for Cp* groups, appearing at δ = 1.92 and 1.96 ppm, respectively.

dx.doi.org/10.1021/ic400432v | Inorg. Chem. 2013, 52, 7923−7932

Scheme 2. Synthesis of Dimolybdaheteroborane Clusters, 7−11[a]

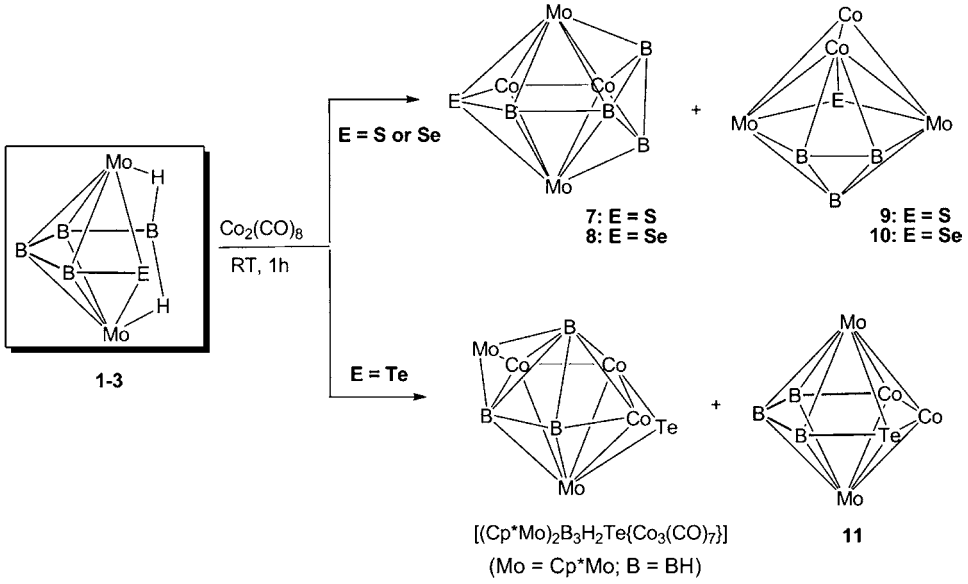

[a]Cross cluster Mo−Mo bonds, Cp* and carbonyl ligands are not shown for clarity.

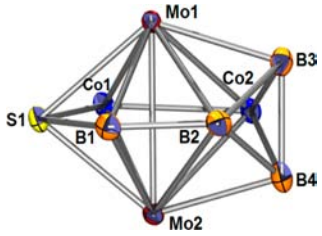

Figure 5. Molecular structure and labeling diagram for **7**. Cp* and Carbonyl ligands are not shown for clarity. Selected bond lengths (Å) and angles (deg): Mo(1)−Mo(2) 2.922, Mo(1)−Co(1) 2.659(9), Co(1)−Co(2) 2.589(11), Mo(1)−B(1) 2.216(7), Co(1)−S(1) 2.228(18), S(1)−B(1) 2.006(7), B(1)−B(2) 1.755(10), B(2)−B(3) 1.735(11), B(2)−B(4) 1.741(11), B(3)−B(4) 1.734(11), B(3)−Co(2) 2.139(8); Mo(1)−Co(1)−Mo(2) 65.5(2), Co(1)−S(1)−B(1) 116.3(2).

The resonances due to BH_t groups are observed in the range between δ 1.36−7.41 ppm. The presence of Cp* and carbonyl ligands were further confirmed by ^{13}C NMR spectra.

Both compounds **7** and **8** are isoelectronic and isostructural with dimetallaborane clusters $[(Cp^*M)_2B_7H_n]$,[24b] [M = W, n = 9; M = Re, n = 7]. Although 9-vertex boron-rich dimetallaborane clusters of W, Re, are reported earlier by Fehlner, both compounds **7** and **8** are the first examples of 9 vertex metal and boron-rich single cage mixed-metallaheteroborane clusters. As shown in Chart 2, various types of 9 vertex *oblatocloso*, *closo*, and *nido* molecular clusters are established.[32,33] Some of them obey the Wade rule,[20] some do not. Cluster **7** is the new entry in this type.

Clusters 9, 10, and 11. Reaction of compounds **1**−**3** with $[Co_2(CO)_8]$ shows a diverse reactivity pattern, which has been reflected in the product distribution. For example, **1**−**2** generated condensed clusters **9** and **10**; however, Te analogue **3** yielded a triple decker sandwich cluster **11**. The compounds have been isolated in low yields. Single crystals suitable for X-ray diffraction analysis of **9**−**11** were obtained from a hexane solution at −4 °C. The X-ray structures confirm the structural inferences made on the basis of spectroscopic results.

The overall structures of **9** (Figure 6) and **10** (Supporting Information, Figure S3) are fascinating, and the core geometry can be viewed as a Mo_2CoB_3 octahedron. The other cobalt atom (Co2) caps the Mo_2Co face of this central Mo_2CoB_3 octahedron consistent with the tendency of transition metals to prefer higher degree vertices. The resulting 7-vertex capped octahedron has a Mo_2Co face involving the Co atom that was used for the first capping process. Capping this face with the single chalcogen atom (E) gives the experimentally observed 8-vertex deltahedron. Clusters **9** and **10** contain 7 sep, required for the octahedron geometry. Thus, **9** and **10** obey the Wade−Mingos electron counting rules for the observed geometry. Clusters **9** and **10** represent an 8-vertex *closo*-metal rich metallaborane containing 70 cluster valence electrons (cve). The pragmatic shape was derived from the *closo*-metal free

Chart 2. 9-Vertex Clusters with Different Geometries

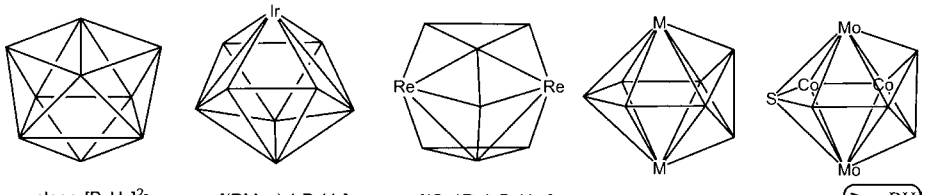

dx.doi.org/10.1021/ic400432v | Inorg. Chem. 2013, 52, 7923−7932

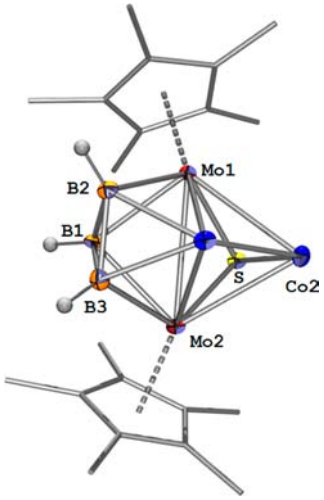

Figure 6. Molecular structure and labeling diagram for **9**. Carbonyl ligands are not shown for clarity. Selected bond lengths (Å) and angles (deg): Mo(1)−Mo(2) 3.008(4), Mo(1)−Co(1) 2.631(5), Co(1)−Co(2) 2.488(6), Mo(1)−B(1) 2.290(4), Mo(1)−S(1) 2.336(7), Co(2)−S(1) 2.220(11), Co(1)−B(2) 2.135(4), B(1)−B(2) 1.697(6), B(3)−Co(1) 2.140(4); B(3)−B(2)−Mo(2) 106.0(19), Co(1)−Co(2)−S(1) 98.87(3).

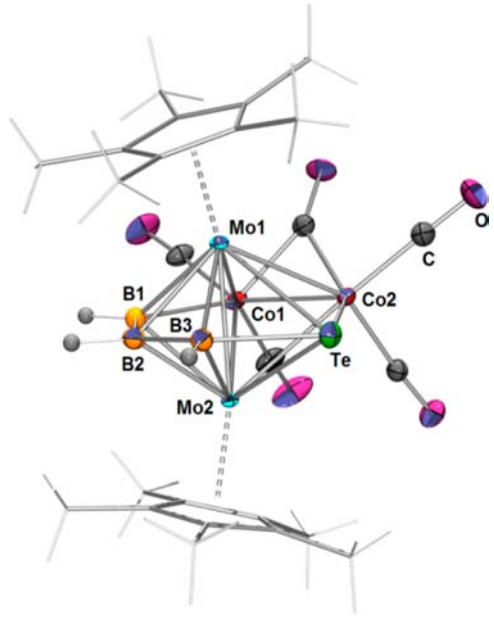

Figure 7. Molecular structure of **11**. Selected bond lengths (Å) and angles (deg): Mo(1)−Mo(2) 2.751(6), Mo(1)−Co(2) 2.655(8), Mo(1)−Te 2.725(6), Mo(2)−Te 2.783, Mo(2)−Co(1) 2.709(9), Co(1)−Co(2) 2.474(10), Mo(2)−B(2) 2.243(7), Co(1)−Te 2.447(8), B(2)−B(3) 1.68(3); Co(1)−Co(2)−Te 114.86(4).

borane deltahedra (dodecahedron) by a diamond-square-diamond (dsd) process, typically generating a degree 6 vertex for the two Mo atoms. The driving force behind this kind of rearrangement is the preference of transition metals for higher-degree vertices than main group atoms.[34] The cross-cluster Mo−Mo distance in **9** and **10** is longer than the usual Mo−Mo single bond distance observed in the molybdaborane $[(Cp^*Mo)_2B_5H_9]$[21] or $[(Cp^*Mo)_2B_4H_6SFe(CO)_3]$,[17a] but comparable with the distances observed in $[(Cp^*Mo)_3MoB_9H_{18}]$[30] and $[(Cp^*Mo)_3B_8H_9]$.[31]

Consistent with the solid state structure (determined by X-ray diffraction), the ^{11}B NMR spectra of **9** and **10** show three boron chemical shifts with intensity ratio of 1:2. The chemical shift at the lower field has been assigned to boron that bridges the two molybdenum metals, and the upfield resonance is assigned to the equivalent boron atoms B(2, 3) connected to two different metals (Mo and Co).

The mild thermolysis of **3** with $[Co_2(CO)_8]$ yielded a byproduct **11**, which is a novel member of the family of known triple-decker complexes. The molecular structure of **11**, shown in Figure 7, contains a planar, hexahapto six-membered ring. To the best of our knowledge, this is the first triple-decker complex in which the middle deck is composed of B, Co, and a heavier group 16 atom (Te). Note that Grimes and co-workers made the first stable and electrically neutral compound in this category in 1973, for example, derivatives of $[Cp_2Co_2C_2B_3H_3]$ which contain a central planar C_2B_3 ring.[18] The molecule **11** possesses a planar (sum of the internal angles 718.46°) six member B_3TeCo_2 ring sandwiched between two Cp*Mo fragments. Although the Mo−B and B−B distances are in the range found for other molybdaboranes characterized,[21] the Co−Te bond length of 2.4471(8) Å is significantly shorter than the corresponding single bond that ranges between 2.575(5)−2.614(5) Å.[35] Thus, the planarity of the ring and its edge lengths are consistent with considering **11** as an analogue of a coordinated benzene just like isolobal $[(CpCr)_2\{\mu\text{-}\eta^6\text{:}\eta^6\text{-}B_4H_4C_2R_2\}]$,[36a] **I**, $[(Cp^*Re)_2\{\mu\text{-}\eta^6\text{:}\eta^6\text{-}1,2\text{-}B_6H_4Cl_2\}]$,[36b] **II** and $[(Cp^*Re)_2\{\mu\text{-}\eta^6\text{:}\eta^6\text{-}B_4H_4Co_2(CO)_5\}]$,[36c] **III**, shown in Chart 3.

Alternatively, the geometry of **11** can be viewed as a hexagonal bipyramid or a dodecahedron, the geometry generally expected for an 8 vertex closo cluster.[37] 9 skeleton electron pairs (sep) are expected to satisfy the electron counting rules for this type of geometry whereas, **11** contains only 6 sep. Thus, the available cluster bonding electrons are inadequate to meet the requirements of a single eight-vertex closo cage. Therefore, compound **11** is better described as a 24-valence electron (ve) triple-decker complex $[(\eta^5\text{-}C_5Me_5Mo)_2\{\mu\text{-}\eta^6\text{:}\eta^6\text{-}B_3H_3TeCo_2(\mu\text{-}CO)(CO)_4\}]$. It is formally an unsaturated 24-electron complex and as such does not obey the "30 and 34-electron rule" put forward by Hoffmann for triple decker sandwiches.

The spectroscopic data of **11** are fully consistent with the solid state structure. The IR spectrum of **11** features strong bands in the range of 2490−2471 cm^{-1} due to terminal B−H stretches and bands in the region of 2028−1816 cm^{-1} due to the presence of terminal and bridging CO ligands. Consistent with the solid state structure (determined by X-ray diffraction), the ^{11}B NMR spectrum shows the presence of three boron atoms at δ = 84.4, 53.5, and 25.9 ppm in the ratio of 1:1:1.

To understand the electronic structure of **11**, the DFT studies were carried out. The structural parameters of **11** were found to be identical to the experimental ones. The molecular orbital study (Figure 8) shows that in the symmetrical η^6:η^6 mode, one of the molybdenum atoms dominates interactions with the B_3TeCo_2 ring in the HOMO. However a good electron delocalization is found perpendicular to the B_3TeCo_2 ring in the energetically well separated HOMO-1, where both the Mo atoms are involved. The WBI (Wiberg Bond Index) value of 0.61 supports the existence of a Mo−Mo cross cluster bond. The localized molecular orbital (LMO) is shown in Figure 8c.

dx.doi.org/10.1021/ic400432v | Inorg. Chem. 2013, 52, 7923−7932

Chart 3. Isoelectronic Triple Decker Sandwich Complexes, I–III and 11

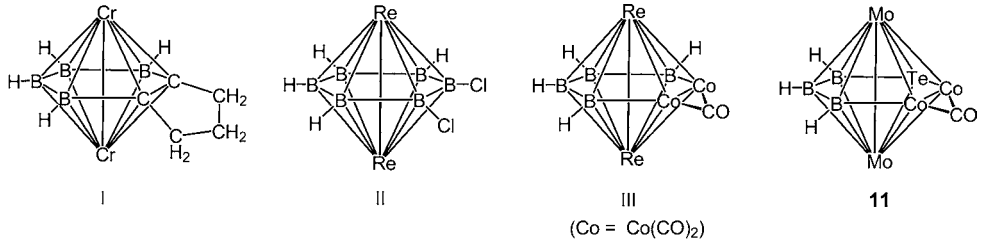

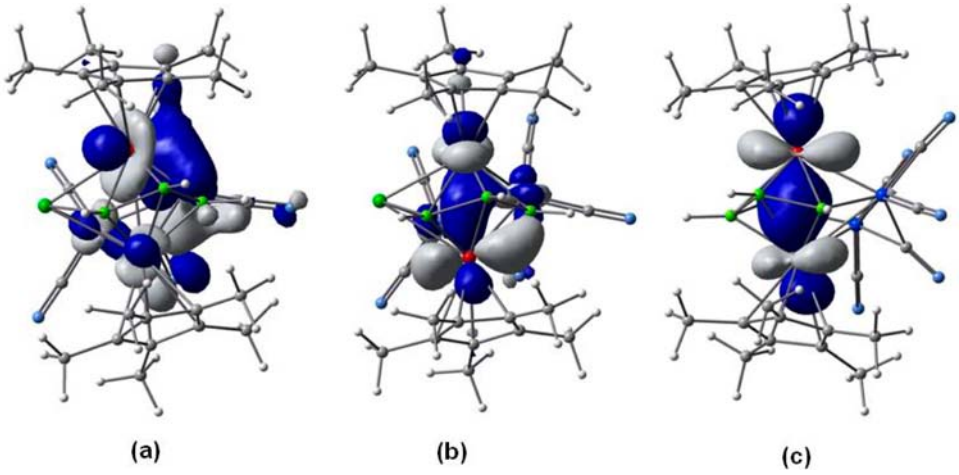

Figure 8. Molecular orbital diagram of **11** (a) HOMO, (b) HOMO-1, and (c) LMO showing Mo–Mo interaction.

CONCLUSION

We report herein the synthesis and structural characterization of a range of dimolybdaheteroborane and tungstaborane clusters and the study of their reactivity with cobalt carbonyl compounds. The results described herein demonstrate that upon replacing the BH_3 fragment by chalcogen atom, the reactivity toward $[Co_2(CO)_8]$ improved drastically. The reactivity of **1–3** with metal carbonyl evidently illustrates the significance of the chalcogen atoms in determining their properties. Cluster **11** is a rare class of 24-electron mixed-metal triple-decker complex containing Te as a cluster constituent. The experimental results were complemented and rationalized by means of DFT studies.

EXPERIMENTAL SECTION

General Procedures and Instrumentation. All the operations were conducted under an Ar/N_2 atmosphere using standard Schlenk techniques or glovebox. Solvents were distilled prior to use under Argon. Cp*H, $[LiBH_4{\cdot}thf]$, selenium powder, tellurium powder, $[Co_2(CO)_8]$, (Aldrich) was used as received. $[(Cp^*Mo)_2B_4H_6E]$,[15,16b] (E = S, Te). Cp^*MoCl_4, Cp^*WCl_4 were prepared according to the reported procedure.[38] The external reference for the ^{11}B NMR, $[Bu_4N(B_3H_8)]$, was synthesized with the literature method.[39] Thin layer chromatography was carried on 250 mm dia aluminum supported silica gel TLC plates (MERCK TLC Plates). NMR spectra were recorded on a 400 MHz Bruker FT-NMR spectrometer. Residual solvent protons were used as reference (δ, ppm, 22 °C, $CDCl_3$, 7.26), while a sealed tube containing $[Bu_4N(B_3H_8)]$ in $[D_6]$ benzene (δ_B, ppm, −30.07) was used as an external reference for the ^{11}B NMR. The resonance frequencies for ^1H, ^{13}C, and ^{11}B NMR has been used as 400, 125, and 128 MHz, respectively. Infrared spectra were recorded on a Nicolet iS10 spectrometer. Microanalyses for C, H, and N were performed on Perkin Elimer Instruments series II model 2400.

Synthesis of 2 and 4–6. In a flame-dried Schlenk tube $[Cp^*MoCl_4]$ (0.5 g, 1.34 mmol) in 10 mL of toluene was treated with 4-fold excess of $[LiBH_4{\cdot}thf]$ (2.7 mL, 5.4 mmol) at −40 °C and allowed to stir at room temperature for 1 h. After removal of toluene, the residue was extracted into hexane and filtered through a frit using Celite. The yellowish-green hexane extract was dried in vacuo, extracted with 15 mL of toluene, and heated at 80 °C with selenium powder (0.22 g, 2.78 mmol) for 20 h. The solvent was evaporated in vacuo; residue was extracted into hexane and passed through Celite mixed with a small amount of silica gel. After removal of solvent from the filtrate, the residue was subjected to chromatographic workup using silica gel TLC plates. Elution with hexane:CH_2Cl_2 (95:05 *v/v*) mixture afforded the following compounds in order of elution: Green $[(Cp^*Mo)_2B_4SeH_6]$, **2** (0.20 g, 25%), $[(Cp^*Mo)_2B_4Se_2H_4]$ (0.08 g, 9%), orange $[(Cp^*Mo)_2B_5H_9]$ (0.16 g, 22%), yellow $[(Cp^*Mo)_2B_5SeH_7]$, **4** (0.06 g, 8%) and orange $[(Cp^*Mo)_2B_6SeH_8]$, **5** (0.09 g, 11%).

Cluster **6** has been synthesized adopting the same reaction procedure for clusters **4** and **5**, using the following chemicals: $[CpWCl_4]$ (0.5 g, 1.27 mmol), $[LiBH_4{\cdot}thf]$ (2.2 mL, 5.08 mmol), and Te powder (0.33 g, 2.54 mmol) to yield $[(CpW)_2B_5Te_2H_5]$, **6** (0.05 g, 7%), and orange $[(CpW)_2B_5H_9]$, (0.14 g, 25%).

2: ^{11}B NMR: δ = 100.7 (d, J_{B-H} = 140 Hz, 1B), 76.7 (d, J_{B-H} = 148 Hz, 1B), 41.8 (d, J_{B-H} = 136 Hz, 1B), 16.8 (d, J_{B-H} = 166 Hz, 1B); ^1H NMR: δ = 8.91 (br, 1B–H_t), 8.12 (br, 1B–H_t), 3.82 (br, 1B–H_t), 2.01 (s, 30H, Cp*), 1.36 (br, 1B–H_t), −10.41 (br, 2Mo-*H*-B); ^{13}C NMR: δ = 106.4 (s, η^5-C_5Me_5), 12.0 (s, η^5-C_5Me_5); IR (hexane, cm^{-1}): 2491 (s) (B–H_t); *Anal.* Calcd (%) for $C_{20}H_{36}B_4Mo_2Se$: C 40.67, H 6.14. Found: C 41.07, H 6.09.

4: ^{11}B NMR: δ = 86.4 (br, 1B), 33.7 (d, 1B), 32.0 (d, 1B), 20.3 (d, 1B), −3.2 (d, 1B); ^1H NMR: δ = 8.54 (br, 1B–H_t), 3.12 (br, 1B–H_t), 3.06 (br, 1B–H_t), 1.91 (s, 30H, Cp*), 1.82 (br, 1B–H_t), −1.21 (br, 1B–H_t), −11.52 (br, 2Mo-*H*-B); ^{13}C NMR: δ = 105.3 (s, η^5-C_5Me_5), 12.9 (s, η^5-C_5Me_5); IR (hexane, cm^{-1}): 2494 (s) (B–H_t).

5: ^{11}B NMR: δ = 95.4 (br, 1B), 78.2 (d, 2B), 14.1 (d, 1B), 6.5 (d, 1B), −10.9 (d, 1B); ^1H NMR: δ = 8.91 (br, 1B–H_t), 8.12 (br, 2B–H_t), 3.82 (br, 1B–H_t), 2.15 (br, 1B–H_t), 1.85 (s, 30H, Cp*), 1.36 (br, 1B–H_t), −9.18 (br, 2Mo-*H*-B); ^{13}C NMR: δ = 103.5 (s, η^5-C_5Me_5),

dx.doi.org/10.1021/ic400432v | *Inorg. Chem.* 2013, 52, 7923–7932

Table 2. Crystallographic Data and Structure Refinement Information for 1, 2, 4−7, and 9−11

	1	2	4	5	6
empirical formula	$0.5(C_{20}H_{36}B_4Mo_2S)+ 0.5(C_{20}H_{37}B_5Mo_2S)$	$C_{20}H_{32}B_4Mo_2Se$	$C_{20}H_{34}B_5Mo_2Se$	$C_{20}H_{38}B_6Mo_2Se$	$C_{10}H_{15}B_5W_2Te_2$
formula weight	549.58	586.54	599.36	598.35	812.15
crystal system	tetragonal	tetragonal	monoclinic	tetragonal	orthorhombic
space group	*P*4(2)/*n*	*P*4(2)/*n*	*P*2(1)/*n*	*P*4(2)/*n*	*Pnma*
a (Å)	22.2242(9)	*24.3557*(3)	10.8520(5)	24.1695(2)	12.8388(5)
b (Å)	22.2242(9)	*24.3557*(3)	16.3337(6)	24.1695(2)	10.4032(4)
c (Å)	8.3666(6)	8.4086(2)	14.7432(6)	8.60720(10)	11.9416(5)
β (deg)	90.00	90.00	110.812(5)	90.00	90.0
V (Å^3)	4909.6(4)	4987.98(15)	2442.77(17)	5028.02(8)	1594.98(11)
Z	8	8	4	8	4
D_{calc} (g/cm^3)	1.487	1.562	1.630	1.581	3.382
F (000)	2232	2320	1188	2368	1388
μ (mm^{-1})	1.110	2.468	10.108	9.821	2.710
θ range (deg)	1.19−24.99	2.37−29.82	2.10−36.04	1.83−33.74	2.33−28.37
goodness-of-fit on F^2	1.234	1.038	1.131	1.046	1.081
R1, *w*R2 [$I > 2\sigma(I)$]	0.0554, 0.1060	0.0675, 0.1732	0.0464, 0.1187	0.0745, 0.1981	0.0415, 0.1325
R1, *w*R2 (all data)	0.0724, 0.1146	0.1601, 0.1732	0.0475, 0.1196	0.0767, 0.2000	0.0511, 0.1422

	7	9	10	11
empirical formula	$C_{25}H_{30}B_4Co_2Mo_2O_5S$	$C_{26}H_{33}B_3Co_2Mo_2O_6S$	$C_{26}H_{33}B_3Co_2Mo_2O_6Se$	$C_{26}H_{33}B_3Co_2Mo_2O_6Te$
formula weight	799.56	815.75	862.65	892.35
crystal system	monoclinic	orthorhombic	orthorhombic	monoclinic
space group	*P*2(1)/*n*	*Pna*2(1)	*Pna*2(1)	*P*2(1)/*c*
a (Å)	9.1308(3)	15.8054(6)	15.8493(5)	17.9134(3)
b (Å)	17.1982(5)	12.0035(3)	12.1257(4)	14.5553(3)
c (Å)	19.1194(7)	15.7935(7)	15.9708(5)	11.3323(2)
β (deg)	97.254(3)	90.00	90.0	98.3480(10)
V (Å^3)	2978.35(17)	2996.34(19)	3069.33(17)	2923.42(9)
Z	4	4	4	4
D_{calc} (g/cm^3)	1.783	1.808	1.867	2.027
F (000)	1592	1624	1696	1730
μ (mm^{-1})	2.021	2.014	3.084	2.968
θ range (deg)	2.87−25.00	2.13−25.00	2.11−25.00	1.15−25.00
goodness-of-fit on F^2	1.110	1.019	1.010	1.061
R1, *w*R2 [$I > 2\sigma(I)$]	0.0615, 0.1653	0.0176, 0.0398	0.0266, 0.0446	0.0342, 0.0824
R1, *w*R2 (all data)	0.0679, 0.1746	0.0192, 0.0407	0.0428, 0.0452	0.0433, 0.0876

11.5 (s, η^5-C_5Me_5); IR (hexane, cm^{-1}): 2496 (s) (B−H$_t$); *Anal.* Calcd (%) for $C_{20}H_{38}B_6Mo_2Se$: C 39.11, H 6.24; found: C 40.01, H 6.18.

6: ^{11}B NMR: δ = 87.2 (br, 1B), 77.5 (d, 1B), 44.1 (br, 2B), −12.0 (d, 1B); ^{1}H NMR: δ = 8.91 (br, 1B−H$_t$), 8.37 (br, 2B−H$_t$), 2.94 (br, 2B−H$_t$), 2.08 (br, 1B−H$_t$), 5.46 (s, 10H, Cp*); ^{13}C NMR: δ = 91.5 (s, Cp); IR (hexane, cm^{-1}): 2448(s) (B−H$_t$), 2491 (s) (B−H$_t$).

General Procedure for the Synthesis of 7−10. A hexane solution of **1** (0.2 g, 0.37 mmol) was added to 3 equivalents of $[Co_2(CO)_8]$ (0.4 g, 1.11 mmol) at room temperature and stirred for 1 h, then volatiles were removed in vacuo and the resulting brown residue was subjected to chromatographic workup using silica gel TLC plates. Elution with hexane:CH_2Cl_2 (70:30 v/v) mixture yielded orange $[(Cp^*Mo)_2B_4H_4SCo_2(CO)_5]$, **7** (0.06 g, 20%), R_f = 0.75 and brown $[(Cp^*Mo)_2B_3H_3SCo_2(CO)_6]$, **9** (0.11 g, 35%), R_f = 0.14. Note that under the similar reaction conditions, **2** (0.2 g, 0.34 mmol) yielded orange $[(Cp^*Mo)_2B_4H_4SeCo_2(CO)_5]$, **8** (0.03 g, 10%), R_f = 0.74 and brown $[(Cp^*Mo)_2B_3H_3SeCo_2(CO)_6]$, **10** (0.07 g, 24%), R_f = 0.15.

7: ^{11}B NMR: δ 102.6 (br, 2B), 77.2 (br, 1B), 35.4 (br, 1B). ^{1}H NMR: δ 7.41 (pcq, 2BH$_t$), 4.72 (s, BH$_t$), 1.92 (s, 30H, 2Cp*), 1.36 (s, BH$_t$). ^{13}C NMR: δ 221.4 (CO), 203.2 (CO), 106.8 (s, 2C_5Me$_5$), 14.26 (s, 2C$_5$*Me*$_5$). IR (hexane) ν/cm^{-1}: 2499 m (BH$_t$), 2031 s, 2009 s, 1985 s (C−O). *Anal.* Calcd (%) for $C_{25}H_{34}B_4Co_2Mo_2O_5S$: C, 37.55; H, 4.29. Found: C, 37.61; H, 4.31.

8: ^{11}B NMR: δ 101.8 (br, 2B), 77.4 (br, 1B), 38.6 (br, 1B). ^{1}H NMR: δ 7.36 (pcq, 2BH$_t$), 3.95 (s, BH$_t$), 1.96 (s, 30H, 2Cp*), 1.38 (s, BH$_t$). ^{13}C NMR: δ 223.8 (CO), 204.7 (CO), 104.6 (s, C_5Me$_5$), 13.9 (s, 2C_5Me$_5$). IR (hexane) ν/cm^{-1}: 2353 m (BH$_t$), 2036 s, 2012 s, 1945 s (C−O).

9: ^{11}B NMR: δ 75.7 (br, 1B), 71.7 (br, 2B); ^{1}H NMR: δ 7.63 (br, BH$_t$), 5.02 (br, 2BH$_t$), 1.92 (s, 30H, 2Cp*); ^{13}C NMR: δ 228.7 (CO), 210.3 (CO), 105.5 (s, C_5Me$_5$), 13.0 ppm (s, C$_5$*Me*$_5$); IR (hexane) ν/cm^{-1} 2497 m (BH$_t$), 2025 (s), 1988(s) ν(C−O). *Anal.* Calcd (%) for $C_{26}H_{33}B_3Co_2Mo_2O_6S$: C 38.28; H 4.08. Found: C, 38.14; H, 3.98.

10: ^{11}B NMR: δ 77.4 (br, 1B), 73.4 (br, 2B); ^{1}H NMR: δ 7.68(br, BH$_t$), 5.27(br, 2BH$_t$), 1.82 (s, 30H, 2Cp*). ^{13}C NMR: δ 219.6 (CO), 201.1 (CO), 104.7 (s, C_5Me$_5$), 13.1 ppm (s, C$_5$*Me*$_5$); IR (hexane) ν/cm^{-1} 2500 m (BH$_t$), 2031 (s), 1992(s) (C−O). *Anal.* Calcd (%) for $C_{26}H_{33}B_3Co_2Mo_2O_6Se$: C 36.20; H, 3.86. Found: C, 36.70; H, 3.97.

Synthesis of 11. In a typical reaction, **3** (0.07 g, 0.10 mmol) in hexane (15 mL) was stirred with 3 equivalents of $[Co_2(CO)_8]$ (0.102 g, 0.30 mmol) for 4 h at 65 °C. The solvent was removed in vacuo; the residue was extracted in hexane, and passed through Celite. The mother liquor was concentrated, and the residue was chromatographed on silica gel TLC plates. Elution with a hexane/CH_2Cl_2 (9:1) mixture yielded brown **11**, (0.007 g, 8%).

11: ^{11}B NMR: δ = 84.4 (br, 1B), 53.5 (br, 1B), 25.9 (br, 1B); ^{1}H NMR: δ = 9.90 (*pcq*, 1BH$_t$), 8.97 (*pcq*, 1BH$_t$), 6.23 (*pcq*, 1BH$_t$), 2.04 (s, 30H, Cp*); ^{13}C NMR: δ = 224.5 (CO), 208.3 (CO), 106.8 (s, η^5-C_5Me$_5$), 12.8 (s, η^5-C$_5$*Me*$_5$); IR (hexane, cm^{-1}): 2490w, 2471m (B−H$_t$), 2028 (s), 1816 (s) ν(C−O); *Anal.* Calc. for $C_{25}H_{33}B_3Co_2Mo_2O_5Te$: C 33.99, H 3.77; found: C 34.11, H 3.58.

Computational Details. Full geometry optimizations were carried out on compounds **1**−**3**, **9**−**11** in gas phase (no solvent effect) using

dx.doi.org/10.1021/ic400432v | *Inorg. Chem.* 2013, 52, 7923−7932

Becke's three parameter hybrid exchange functional (B3LYP)[40] in combination with the nonlocal correlation functional provided by the Lee–Yang–Parr expression,[41] which combines the Hartree–Fock exchange term with the DFT exchange-correlation terms. To assess the nature of the stationary point on the potential energy surface we performed additional harmonic frequency calculations at the same level of theory on the optimized geometry. A sufficiently flexible basis set expansion, all electron double-ζ valence basis set denoted by 6-311++G(3d,2p) or DGDZVP was used for all non metallic atoms, for example, carbon, oxygen, boron, sulfur, and selenium. We adopted Stuttgart/Dresden double-ζ (SDD) effective core potentials (ECPs)[42] for Mo, Te, and Co atoms. The crystallographic coordinates were used as a starting geometry for complete geometry optimizations. We also computed NMR shielding tensors at the B3LYP/GIAO[43−46] level of theory. TMS ($SiMe_4$) was used as internal standard for the ^1H NMR chemical shift calculations. The ^{11}B NMR chemical shifts were calculated relative to B_2H_6 (B3LYP B shielding constant 81.4 ppm) and converted to the usual $BF_3{\cdot}OEt_2$ scale using the experimental $\delta(^{11}B)$ value of B_2H_6, 16.6 ppm.[47] All the quantum-chemical calculations were carried out using density functional theory (DFT) as implemented in the Gaussian 09[48] program package. Further, NBO analysis was carried out using the NBO routine within the Gaussian 09 package.

X-ray Structure Determination. Crystallographic information for **1**, **2**, **4**−**7**, and **9**−**11** are shown in Table 2. Crystal data for **4**−**7** were collected and integrated using OXFORD DIFFRACTION XCALIBUR-S CCD system equipped with graphite-monochromated Mo Kα radiation (λ = 0.71073 Å) radiation at 150 K. The crystal data for **1**, **2**, and **9**−**11** were collected and integrated using a Bruker AXS kappa apex2 CCD diffractometer, with graphite monochromated Mo−Kα (λ = 0.71073 Å) radiation at 248 K. The structures were solved by heavy atom methods using SHELXS-97 or SIR92 and refined using SHELXL-97 (Sheldrick, G.M., University of Göttingen).[49,50]

■ ASSOCIATED CONTENT

Supporting Information

X-ray crystallographic files in CIF format for **1**, **2**, **4**−**7**, and **9**−**11**. This material is available free of charge via the Internet at http://pubs.acs.org.

■ AUTHOR INFORMATION

Corresponding Author

*E-mail: sghosh@iitm.ac.in.

Notes

The authors declare no competing financial interest.

■ ACKNOWLEDGMENTS

Generous support of the Indo-French Centre for the Promotion of Advanced Research (IFCPAR-CEFIPRA), No.4405-1, New Delhi is gratefully acknowledged. K.K.C is grateful to UGC and A.T is grateful to CSIR, India, for a Research Fellowship. B.M. thanks the Indian Institute of Technology Madras, India, for a Research Fellowship.

■ REFERENCES

(1) (a) Fehlner, T. P.; Halet, J.-F.; Saillard, J.-Y. *Molecular Clusters: A Bridge to Solid-State Chemistry*; Cambridge University Press: Cambridge, U.K., 2007. (b) Braunschweig, H.; Colling, M. *Coord. Chem. Rev.* **2001**, *223*, 1.

(2) (a) Mathur, P.; Sekar, P.; Satyanarayana, C. V. V; Mahon, M. F. *J. Chem. Soc., Dalton Trans.* **1996**, 2173. (b) Gray, T. G. *Coord. Chem. Rev.* **2003**, *243*, 213. (c) Shieh, M.; Chung, R.-L.; Yu, C.-H.; Hsu, M.-H.; Ho, C.-H.; Peng, S.-M.; Liu, Y.-H. *Inorg. Chem.* **2003**, *42*, 5477.

(3) Whitmire, K. H. *J. Coord. Chem.* **1998**, *17*, 95.

(4) (a) Braunschweig, H. *Angew. Chem., Int. Ed.* **1998**, *37*, 1786. (b) Ghosh, S.; Lei, X.; Shang, M.; Fehlner, T. P. *Inorg. Chem.* **2000**, *39*, 5373. (c) Ghosh, S.; Shang, M.; Fehlner, T. P. *J. Organomet. Chem.* **2000**, *614*−*615*, 92.

(5) (a) Greenwood, N. N.; Ward, I. M. *Chem. Soc. Rev.* **1974**, *3*, 231. (b) Grimes, R. N. *Acc. Chem. Res.* **1978**, *11*, 420. (c) Grimes, R. N. *Pure Appl. Chem.* **1982**, *54*, 43. (d) Grimes, R. N. In *Metal Interactions with Boron Clusters*; Grimes, R. N., Ed.; Plenum: New York, 1982; p 269.

(6) (a) Kennedy, J. D. *Prog. Inorg. Chem.* **1984**, *32*, 519. (b) Kennedy, J. D. *Prog. Inorg. Chem.* **1986**, *34*, 211.

(7) (a) Barton, L.; Srivastava, D. K. In *Comprehensive Organometallic Chemistry II*; Wilkinson, G., Abel, E. W., Stone, F. G. A., Eds.; Pergamon Press: Elmsford, NY, 1995; Vol. *1*, Chapter 8, p 275. (b) Grimes, R. N. In *Comprehensive Organometallic Chemistry II*; Wilkinson, G., Abel, E. W., Stone, F. G. A., Eds.; Pergamon Press: Elmsford, NY, 1995; Vol *1*, Chapter 9, p 374. (c) Grimes, R. N. *Carboranes*, 2nd ed.; Elsevier Inc.: Amsterdam, The Netherlands, 2011.

(8) (a) Briguglio, J. J.; Sneddon, L. G. *Organometallics* **1985**, *4*, 721. (b) Kadlecek, D. E.; Carroll, P. J.; Sneddon, L. G. *J. Am. Chem. Soc.* **2000**, *122*, 10868. (c) Jan, D.-Y.; Workman, D. P.; Hsu, L.-Y.; Krause, J. A.; Shore, S. G. *Inorg. Chem.* **1992**, *31*, 5123. (d) Kealy, T. J.; Pauson, P. L. *Nature* **1951**, *168*, 1039.

(9) (a) Meng, X.; Bandyopadhyay, A. K.; Fehlner, T. P.; Grevels, F.-W. *J. Organomet. Chem.* **1990**, *394*, 15. (b) Bose, S. K.; Geetharani, K.; Ramkumar, V.; Varghese, B.; Ghosh, S. *Inorg. Chem.* **2010**, *49*, 2881. (c) Ghosh, S.; Noll, B. C.; Fehlner, T. P. *Angew. Chem., Int. Ed.* **2005**, *44*, 2916.

(10) (a) Fehlner, T. P. *J. Chem. Soc., Dalton Trans.* **1998**, 1525. (b) Fehlner, T. P. *Organometallics* **2000**, *19*, 2643. (c) Ghosh, S.; Rheingold, A. L.; Fehlner, T. P. *Chem. Commun.* **2001**, 895.

(11) (a) Burke, A.; Ellis, D.; Giles, B. T.; Hodson, B. E.; Macgregor, S. A.; Rosair, G. M.; Welch, A. J. *Angew. Chem., Int. Ed.* **2003**, *42*, 225. (b) Burke, A.; Ellis, D.; Ferrer, D.; Ormbsy, D. L.; Rosair, G. M.; Welch, A. J. *Dalton. Trans.* **2005**, 1716.

(12) (a) Deng, L.; Zhang, J.; Chan, H.-S.; Xie, Z. *Angew. Chem., Int. Ed.* **2006**, *45*, 4309. (b) Deng, L.; Xie, Z. *Coord. Chem. Rev.* **2007**, *251*, 2452. (c) Zhang, J.; Chan, H.-S.; Xie, Z. *Angew. Chem., Int. Ed.* **2008**, *47*, 9447.

(13) Roy, D. K.; Bose, S. K.; Anju, R. S.; Mondal, B.; Ramkumar, V.; Ghosh, S. *Angew. Chem., Int. Ed.* **2013**, *52*, 3222.

(14) (a) Geetharani, K.; Tussupbayev, S.; Borowka, J.; Holthausen, M. C.; Ghosh, S. *Chem.—Eur. J.* **2012**, *18*, 8482. (b) Yan, H.; Beatty, A. M.; Fehlner, T. P. *Angew. Chem., Int. Ed.* **2001**, *40*, 4498.

(15) (a) Roy, D. K.; Bose, S. K.; Geetharani, K.; Chakrahari, K. K. V.; Mobin, S. M.; Ghosh, S. *Chem.—Eur. J.* **2012**, *18*, 9983. (b) Bose, S. K.; Geetharani, K.; Ramkumar, V.; Mobin, S. M.; Ghosh, S. *Chem.—Eur. J.* **2009**, *15*, 13483. (c) Geetharani, K.; Bose, S. K.; Varghese, B.; Ghosh, S. *Chem.—Eur. J.* **2010**, *16*, 11357. (d) Sahoo, S.; Dhayal, R. S.; Varghese, B.; Ghosh, S. *Organometallics* **2009**, *28*, 1586.

(16) (a) Geetharani, K.; Bose, S. K.; Sahoo, S.; Ghosh, S. *Angew. Chem., Int. Ed.* **2011**, *50*, 3908. (b) Thakur, A.; Sao, S.; Ramkumar, V.; Ghosh, S. *Inorg. Chem.* **2012**, *51*, 8322.

(17) (a) Chakrahari, K. K. V.; Ghosh, S. *J. Chem. Sci.* **2011**, *123*, 847. (b) Krishnamoorthy, B. S.; Thakur, A.; Chakrahari, K. K. V.; Bose, S. K.; Hamon, P.; Roisnel, T.; Kahlal, S.; Ghosh, S.; Halet, J.-F. *Inorg. Chem.* **2012**, *51*, 10375. (c) Thakur, A.; Chakrahari, K. K. V.; Mondal, B.; Ghosh, S. *Inorg. Chem.* **2013**, *52*, 2262.

(18) (a) Grimes, R. N. *Collect. Czech. Chem. Commun.* **2002**, *67*, 728. (b) Beer, D. C.; Miller, V. R.; Sneddon, L. G.; Grimes, R. N.; Mathew, M.; Palenik, G. J. *J. Am. Chem. Soc.* **1973**, *95*, 3046. (c) Grimes, R. N.; Beer, D. C.; Sneddon, L. G.; Miller, V.; Weiss, R. *Inorg. Chem.* **1974**, *13*, 1138.

(19) (a) Sahoo, S.; Mobin, S. M.; Ghosh, S. *J. Organomet. Chem.* **2010**, *695*, 945. (b) Dhayal, R. S.; Ramkumar, V.; Ghosh, S. *Polyhedron* **2010**, *30*, 2062.

(20) (a) Mingos, D. M. P. *Nature (London)* **1972**, *236*, 99. (b) Wade, K. *New Scientist* **1974**, *62*, 615. (c) Wade, K. Adv. *Inorg. Chem. Radiochem.* **1976**, *18*, 1. (d) Mingos, D. M. P. *J. Chem. Soc., Chem. Commun.* **1983**, 706.

(21) (a) Kim, D. Y.; Girolami, G. S. *J. Am. Chem. Soc.* **2006**, *128*, 10969. (b) Aldridge, S.; Shang, M.; Fehlner, T. P. *J. Am. Chem. Soc.* **1998**, *120*, 2586.
(22) Dhayal, R. S.; Chakrahari, K. K. V.; Varghese, B.; Mobin, S. M.; Ghosh, S. *Inorg. Chem.* **2010**, *49*, 7741.
(23) Dhayal, R. S.; Ponniah, S. J.; Sahoo, S.; Ghosh, S. *Indian J. Chem.* **2011**, *50A*, 1363.
(24) (a) Weller, A. S.; Shang, M.; Fehlner, T. P. *Chem. Commun.* **1998**, 1787. (b) Weller, A. S.; Shang, M.; Fehlner, T. P. *Organometallics* **1999**, *18*, 853. (c) Bose, S. K.; Ghosh, S.; Noll, B. C.; Halet, J.-F.; Saillard, J.-Y.; Vega, A. *Organometallics* **2007**, *26*, 5377.
(25) Bicerano, J.; Lipscomb, W. N. *Inorg. Chem.* **1980**, *19*, 1825.
(26) Dolansky, J.; Hermanek, S.; Zahradnik, R. *Collect. Czech. Chem. Commun.* **1981**, *46*, 2479.
(27) (a) Bashirov, D. A.; Fuhr, O.; Konchenkoa, S. N. *Russ. Chem. Bull., Int. Ed.* **2006**, *55*, 802. (b) Adams, C. J.; Bruce, M. I.; Skelton, B. W.; White, A. H. *Inorg. Chem.* **1992**, *31*, 3336. (c) Pergola, D. R.; Garlaschelli, L.; Manassero, M.; Sansoni, M. *J. Cluster Sci.* **1999**, *10*, 109.
(28) Geetharani, K.; Bose, S. K.; Sahoo, S.; Varghese, B.; Mobin, S. M.; Ghosh, S. *Inorg. Chem.* **2011**, *50*, 5824.
(29) (a) Housecroft, C. E. *Boranes and Metalloboranes*; Ellis Horwood: Chichester, U.K., 1990. (b) Shriver, D. F., Kaesz, H. D., Adams, R. D., Eds. *The Chemistry of Metal Cluster. Complexes*; VCH: New York, 1990. (c) Ghosh, S.; Fehlner, T. P.; Noll, B. C. *Chem. Commun.* **2005**, 3080.
(30) Dhayal, R. S.; Sahoo, S.; Reddy, K. H. K.; Mobin, S. M.; Jemmis, E. D.; Ghosh, S. *Inorg. Chem.* **2010**, *49*, 900.
(31) Chakrahari, K. K. V.; Thakur, A.; Mondal, B.; Dhayal, R. S.; Ramkumar, V.; Ghosh, S. *J. Organomet. Chem.* **2012**, *710*, 75.
(32) Bould, J.; Crook, J. E.; Greenwood, N. N.; Kennedy, J. D.; McDonald, W. S. *J. Chem. Soc., Chem. Commun.* **1982**, 346.
(33) Bould, J.; Harrington, R. W.; Clegg, W.; Kennedy, J. D. *J. Organomet. Chem.* **2012**, *721*−*722*, 155.
(34) King, R. B. *Inorg. Chem.* **2006**, *45*, 8211.
(35) Steigerwald, M. L.; Siegrist, T.; Stuczynski, S. M. *Inorg. Chem.* **1991**, *30*, 4940.
(36) (a) Kawamur, K.; Shang, M.; Wiest, O.; Fehlner, T. P. *Inorg. Chem.* **1998**, *37*, 608. (b) Ghosh, S.; Shang, M.; Fehlner, T. P. *J. Am. Chem. Soc.* **1999**, *121*, 7451. (c) Ghosh, S.; Beatty, A. M.; Fehlner, T. P. *J. Am. Chem. Soc.* **2001**, *123*, 9188.
(37) (a) Williams, R. E. *Inorg. Chem.* **1971**, *10*, 210. (b) Rudolph, R. W. *Acc. Chem. Res.* **1976**, *9*, 446. (c) Mingos, D. M. P.; Wales, D. J. *Introduction to Cluster Chemistry*; Prentice Hall: New York, 1990.
(38) Green, M. L. H.; Hubert, J. D.; Mountford, P. *J. Chem. Soc., Dalton Trans.* **1990**, 3793.
(39) Ryschkewitsch, G. E.; Nainan, K. C. *Inorg. Synth.* **1974**, *15*, 113.
(40) Lee, C.; Yang, W.; Parr, R. G. *Phys. Rev. B* **1988**, *37*, 785.
(41) Sorkin, A.; Truhlar, D. G.; Amin, E. A. *J. Chem. Theory Comput.* **2009**, *5*, 1254.
(42) Dolg, M.; Stoll, H.; Preuss, H. *Theor. Chim. Acta* **1993**, *85*, 441.
(43) Schreckenbach, G.; Ziegler, T. J. *J. Phys. Chem.* **1995**, *99*, 606.
(44) Schreckenbach, G.; Ziegler, T. J. *Int. J. Quantum Chem.* **1997**, *61*, 899.
(45) Schreckenbach, G.; Ziegler, T. J. *Int. J. Quantum Chem.* **1996**, *60*, 753.
(46) Wolff, S. K.; Ziegler, T. J. *J. Chem. Phys.* **1998**, *109*, 895.
(47) Onak, T. P.; Landesman, H. L.; Williams, R. E.; Shapiro, I. *J. Phys. Chem.* **1959**, *63*, 1533.
(48) Frisch, M. J.; Trucks, G. W.; Schlegel, H. B.; Scuseria, G. E.; Robb, M. A.; Cheeseman, J. R.; Scalmani, G.; Barone, V.; Mennucci, B.; Petersson, G. A.; Nakatsuji, H.; Caricato, M.; Li, X.; Hratchian, H. P.; Izmaylov, A. F.; Bloino, J.; Zheng, G.; Sonnenberg, J. L.; Hada, M.; Ehara, M.; Toyota, K.; Fukuda, R.; Hasegawa, J.; Ishida, M.; Nakajima, T.; Honda, Y.; Kitao, O.; Nakai, H.; Vreven, T.; Montgomery, J. A.; Jr.; Peralta, J. E.; Ogliaro, F.; Bearpark, M.; Heyd, J. J.; Brothers, E.; Kudin, K. N.; Staroverov, V. N.; Keith, T.; Kobayashi, R.; Normand, J.; Raghavachari, K.; Rendell, A.; Burant, J. C.; Iyengar, S. S.; Tomasi, J.; Cossi, M.; Rega, N.; Millam, J. M.; Klene, M.; Knox, J. E.; Cross, J. B.; Bakken, V.; Adamo, C.; Jaramillo, J.; Gomperts, R.; Stratmann, R. E.; Yazyev, O.; Austin, A. J.; Cammi, R.; Pomelli, C.; Ochterski, J. W.; Martin, R. L.; Morokuma, K.; Zakrzewski, V. G.; Voth, G. A.; Salvador, P.; Dannenberg, J. J.; Dapprich, S.; Daniels, A. D.; Farkas, O.; Foresman, J. B.; Ortiz, J. V.; Cioslowski, J.; Fox, D. J. *Gaussian 09*, Revision C.01; Gaussian, Inc.: Wallingford, CT, 2010.
(49) Sheldrick, G. M. *SHELXS-97*; University of Göttingen: Göttingen, Germany, 1997.
(50) Sheldrick, G. M. *SHELXL-97*; University of Göttingen: Göttingen, Germany, 1997.